STUDY OF RADIATIVE RECOMBINATION AND DIELECTRONIC RECOMBINATION PROCESSES FOR (F XII–F IX , Na IX–Na XI , Mg X-Mg XII , Ni XXVI-Ni XXVIII) IONS

Alaa A. Khalaf

Department of Physics-College of Science-Basrah University

Email: alaa75uob@hotmail.com

ABSTRACT

An investigation has been carried out of radiative recombination process for (F^{7+}- F^{9+}, Na^{9+}- Na^{11+}, Mg^{10+}-Mg^{12+}, Ni^{26+}- Ni^{28+}) ions, and dielectronic recombination for (F^{7+}, Na^{9+}, Mg^{10+}) ions, by calculating the rate coefficient for those processes, which is important in understanding ionization balance in both laboratory and astrophysical plasmas. In this paper we compare recombination rate coefficients given by empirical formulas with the data of other researchers. In general the agreement was very good and the considerable conclusion that the resonance in the rate coefficients of dielectronic channels decreases for highly charged ions.

Keywords- Cross sections, Recombination rate, Electron-ion interaction.

دراسة عمليات اعادة الاتحاد المشع وثنائي الالكترون للآيونات

(F XII–F IX , Na IX–Na XI , Mg X−Mg XII , Ni XXVI−Ni XXVIII)

أ.م.د.علاء عبد الحسن خلف

قسم الفيزياء – كلية العلوم – جامعة البصرة

الخلاصة

قمنا باجراء بحث يتناول عملية اعادة الاتحاد المشع للآيونات (F^{7+}– F^{9+}، Na^{9+}– Na^{11+}، Mg^{10+}– Mg^{12+}، Ni^{26+}– Ni^{28+}) واعادة الاتحاد ثنائي الألكترون للآيونات(F^{7+}, Na^{9+}, Mg^{10+}) من خلال حساب معامل المعدل لهذه العمليات، والذي يكون بدوره مهما في فهم التوازن الايوني في كل من مختبرات الابحاث والبلازما الفلكية. في هذا البحث قمنا بمقارنة معدل معاملات اعادة الاتحاد المستحصلة من صيغ تجريبية مع قراءات باحثين اخرين. بصورة عامة كان التوافق بين حساباتنا وقراءات الباحثين جيده جدا وقد استنتجنا من هذه الحسابات ان الرنين في معدل المعاملات لقنوات ثنائية الألكترون يتضائل للآيونات عالية الشحنة.

كلمات مفتاحية– مقاطع عرضية، معدل اعادة الاتحاد، تفاعل الكترون– آيون

Introduction

There are many mechanisms of electron-ion collision, which are very important in plasma, as example ionization, excitation and recombination. These processes can take place directly in one step by single interaction or indirectly in two steps or more [1]. There combination of electrons with ions is very interesting because of the possibilities of high resolution measurements and because of the need of atomic data in plasma and astrophysical research [2].

Plasma is the fourth state of the matter and it is supposed to be the most common and abundant form of matter in universe [3]. One of the most important subjects of plasmas is the emission of radiation, which has a principal rule in determining the properties of plasma such as ionization balance, density, temperature and elemental abundances. As a result, this emission takes place the electron-ion interaction processes such as excitation, ionization, and electron-ion recombination process [4].

Electron-ion is a very high exothermic process in which the atomic ion capture an electron after collision. When the densities of the electron be low and moderate, there are two channels of recombination through which the atomic ion recombine with a free electron, those two processes are radiative recombination (RR) and dielectronic recombination (DR). The radiative recombination is a non-resonant channel and classified as a mechanism of direct mode, while dielectronic recombination is indirect resonant mode working in two steps. In both processes the excess energy and momentum of captured electron are taken away by the emitted photon [1].

The radiative recombination (RR) is a one step direct channel in which energy liberated by the binding of the free electron is carried away by a photon instantly [2], as shown in fig.(1-a).

$$e + A^{q+} \rightarrow A^{(q-1)+} + photon$$

The dielectronic recombination (DR) involves two steps. In the first step a free electron is captured by the atomic ion with a simultaneous excitation of a second electron bound to the ion. In the second step the new charge state of the ion is stabilized by emitting of a photon [2], as shown in fig.(1-b).

$$e + A^{q+} \rightarrow [A^{(q-1)+}]^{**} \rightarrow A^{(q-1)+} + photon$$

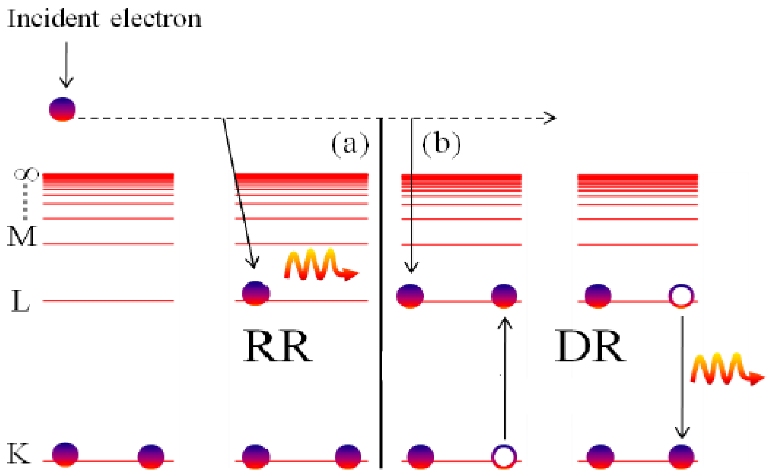

Figure(1): Schematic diagram[1] of:
(a) Radiative recombination
(b) Dielectronic recombination in He-like ion

In plasma collisions happens between ions with each others or with electrons. Many types of reactions can be included as a result of that, for example ionization and recombination, each process need to be studied separately to understand the behavior of plasma [1].

The dielecronic recombination (DR), is the process which governs the charge balance state in plasma. The coefficient rate of dielectronic recombination form the principal ingredient in the modeling codes of plasma that are employed for the analysis of spectra obtained from astrophysical observations [5].

The accuracy of rate coefficients for the atomic collision processes is required, in order to be able to estimate a rational description of the plasma properties, such as element abundances and temperatures. To date most DR rate coefficients are used for the modeling stem of plasma from theoretical calculations [6].

In electron-ion interactions the charge changing being crucially important in plasmas, whether of man made or astrophysical nature. As they play principal rule in estimating the ionization balance and the properties of plasma. One needs the atomic collision data, such as rate coefficient, resonance energy positions, and recombination cross sections for diagnosing and modeling the state of high temperature plasma [1].

Many investigations have been carried out by many researchers for RR and DR processes [7-14]. Two powerful experimental techniques has been depended in this field; The Electron Beam Ion Source and Traps (EBIS-Ts) [15-17] and Heavy-Ion Storage rings [18-20].

Theory

Radiative recombination (RR) and dielectronic recombination (DR) are fundamental channel processes with great influence on the charge state balance of the atomic ions in plasma and on the radiation emitted. Therefore, as a result, rate coefficient data for these channels are needed for understanding and diagnostics as well as modeling of all plasmas.

In this paper we depend the formula of radiative recombination rate coefficients for both ground and metastable levels, for Gu [21], which were fitted to the usual functional form:

$$\alpha_{RR}(T) = A\left[\sqrt{T/T_0}(1+\sqrt{T/T_0})^{1-B}(1+\sqrt{T/T_1})^{1+B}\right]^{-1} \quad \ldots\ldots\ (1)$$

Where $\alpha_{RR}(T)$ is in unit ($cm^3\ s^{-1}$). Here T_0 , T_1 are in units of temperature (*K*), the unit of *A* is ($cm^3\ s^{-1}$) while *B* dimensionless. Table (1) presents the fitting parameters, where a nonlinear least-square fit has been used to determine the coefficients [22].

The dependent formula for determining dielectronic recombination rate $\alpha_{DR}(T)$ [23, 24] is:

$$\alpha_{DR}(T) = \frac{1}{T^{3/2}}\sum_{i=1}^{k} C_i \exp(-\frac{E_i}{T}) \quad \ldots\ldots\ (2)$$

Where C_i is in unit $K^{3/2}cm^3s^{-1}$ the resonance strength for the *ith* fitting component and E_i are in unit *K*, the corresponding energy parameter. In table (2) we present C_i and E_i [23] for atomic ions under investigation to calculate $\alpha_{DR}(T)$.

Results & discussion

It's well-known that Radiative recombination rate coefficients are required in estimating the balance of ionization in plasmas resulting from thermodynamic equilibrium, as is often the case in environments of astrophysics. Although, it is convenient to separate the channels of recombination into the non-resonant radiative recombination (RR) and the resonant dielectronic recombination (DR).

A survey will explore our results of radiative recombination rate coefficients $\alpha_{RR}(T)$ as a function of electron temperature for (F^{7+}, F^{8+}, F^{9+}, Na^{9+}, Na^{10+}, Na^{11+}, Mg^{10+}, Mg^{11+}, Mg^{12+}, Ni^{26+}, Ni^{27+}, Ni^{28+}) ions, and also will explore our results of dielectronic recombination rate coefficients $\alpha_{DR}(T)$ as a function of electron temperature for (F^{7+}, Na^{9+}, Mg^{10+}) ions.

Figures (1), (3), (5) shows our results of radiative recombination rate coefficients $\alpha_{RR}(T)$ for (F^{7+}, F^{8+}, F^{9+}) ions compared with the theoretical data of Verner & Ferland [25] and Nahar [26], whereas in figures (2), (4) we presents the same of figures (1), (3) alternatively, by taking a logarithmic scale for the rate coefficient, with a purpose to illustrate the resonance action in Nahar data which appears at high temperatures. Nahar [26] used the unified method for total electron-ion recombination account for both radiative and dielectronic recombination processes in an *ab initio* manner provides a single set of recombination rate coefficients [27]. In the subsequent figures we will review the action of (DR) for ions under investigation.

In figures (6), (8), (10) and (11), (13), (15), we presents our calculations of $\alpha_{RR}(T)$ for (Na^{9+}, Na^{10+}, Na^{11+}) and (Mg^{10+}, Mg^{11+}, Mg^{12+}) ions alternatively, which in turn compared with the theoretical data of Verner & Ferland [25] and Nahar [27], also here figures (7), (9) and (12), (14) represent the same of figures (6), (8) and (11), (13) alternatively, in logarithmic scale.

In figures (16), (17), (18) we presents our calculations of radiative recombination rate coefficients $\alpha_{RR}(T)$ for (Ni^{26+}, Ni^{27+}, Ni^{28+}) ions compared with the theoretical data of Verner & Ferland [25] and Nahar [28]. Finally, in figures (19), (20), (21), and (22) we present our results of the dielectronic recombination rate coefficients $\alpha_{DR}(T)$ for (F^{7+}, Na^{9+}, Mg^{10+}) ions compared with the theoretical data of Nahar [26, 27].

In general our obtained results of $\alpha_{RR}(T)$ and $\alpha_{DR}(T)$ give a very good agreement with all the data that has compared with. The disagreement happened between our results for $\alpha_{RR}(T)$ and Nahar data at a small period of the high electron temperature, and as we mention that the unified method used by Nahar combine between the resonant and non-resonant channels was what caused this disagreement. Our calculations of $\alpha_{DR}(T)$ made for electron temperature range (10^6-10^9) *K*, where the resonance appears only at high temperatures, the agreement was good and the behavior of the curves was similar.

Conclusion

Vast quantities of electron-ion collisions are necessary to collect and get precise information about the energy balance, structure, and temperature distribution etc of these astrophysical aspects.

From what presented by exploring our results of radiative and dielectronic recombination rate coefficients we conclude the following; first, when the charge of the ion increases the probability of the appearance of resonance is decreasing as we see in Fluorine ions where only in F^{7+} and F^{8+} there was a resonance rising at high temperatures where the effects of dielectronic channel begin to appears, but there was no resonance for F^{9+} ion. The same thing happens with (Na^{9+}, Na^{10+}, Na^{11+}) and (Mg^{10+}, Mg^{11+}, Mg^{12+}) ions. Second, the highly charged ions like Nickel (Ni^{26+}, Ni^{27+}, Ni^{28+}) all shows no resonance rising and this support our conclusion that when the charge of the ion increases the resonance appearances decreases.

REFERENCES

[1]. S. Ali, "**Electron-ion recombination data for plasma application"**, PhD Thesis: Stockholm University (2012).

[2]. A. Muller et.al, **"Recent dielecronic recombination experiments"** Hyp. Int. Vol. 114, (1998), PP. 229-235.

[3]. J. A. Bittencourt, **"Fundumental of plasma physics"** 3rd edition, springer-verlag New York Inc. (2004).

[4]. Y. Hahn, **"Electron-ion recombination processes-an review** Rep. Prog. Phys. Vol. 60, (1997), PP. 691-759.

[5]. G. J. Ferland, **"Quantitative spectroscopy of photoionized clouds"** Annu. Rev. Astron. Astrophys. Vol. 41, (2003), PP. 517-554.

[6]. S. Bohm, A. Muller, S. Schippers, W. Shi, M. Fogle, P. Glans, R. Schuch, and H. Danared, **"Experimental N v and Ne viii low-temperature dielectronic recombination rate coefficient"** A & A Vol. 437, (2005), PP. 1151-1157.

[7]. I. Orban, P. Glans Z. Altun, E. Lindroth, A. Kallberg, and R. Schuch, **"Determination of the recombination rate coefficients for Na-like Si iv forming Mg-like Si iii"** A & A Vol. 459, (2006), PP. 291-296.

[8]. M. B. Trzhaskovskaya, V. K. Nikulin, and R. E. H. Clark, **"Multipole and relativistic effects in radiative recombination process in hot plasmas"** Phys. Rev. E Vol. 78, (2008), PP. 035401(4).

[9]. E. W. Schmidt, S. Schippers, D. Bernhardt, A. Muller, J. Hoffmann, M. Lestinsky, D. A. Orlv, A. Wolf, D. V. Lukic, D. W. Savin, and N. R. Badnell, **"Electron-ion recombination for Fe VIII forming Fe VII and Fe IX forming Fe VIII:measurements and theory"** A & A Vol. 492, (2008), PP. 265-275.

[10]. S. Schippers, M. Lestinsky, A. Muller, D. w. Savin, E. W. Schmidt, and A. Wolf, **"Electron-ion recombination for Fe VIII forming Fe VII and Fe IX forming Fe VIII: measurements and theory"** Int. Rev. At. Mol. Phys. Vol 1, (2010), PP. 109-121.

[11]. S. Hamasha, A. Naser, **"Developing a comprehensive atomic utility program enhanced with a hydrogenic model for plasma and astrophysics applications"** J. Appl. Sci. Vol 11, (2011), PP. 3413-3420.

[12]. D. Bernhardt, A. Becker, M. Grieser, M. Hahn, C. Krantz, M. Lestinsky, O. Novotny, R. Repnow, D. W. Savin, K. Spruck, A. Wolf, A. Muller, and S. Schippers, **“Absolute rate coefficients for photorecombination and electron-impact ionization of magnesiumlike iron ions from measurements at a heavy-ion storage ring”** Phys. Rev. A Vol 90, (2014), PP. 012702(11).

[13]. M. F. Gu, **“Dielectronic recombination rate coefficients for H-like through Ne-like isosequences of Mg, Si, S, Ar, Ca, Fe, and Ni”** ApJ **590**, (2003), PP. 1131-1140.

[14]. M. Lestinsky, N. R. Badnell, D. Bernhardt, M. Grieser, J. Hoffimann, D. Lukic, A. Muller, D. A. Orlov, R. Repnow, D. W. Savin, E. W. Schmidt, M. Schnell, S. Schippers, A. Wolf, and D. Yu, **“Electron-ion recombination of Fe X forming Fe IX and of Fe XI forming Fe X: Laboratory measurements and theoretical calculations”** ApJ Vol. 698, (2009), PP. 648-659.

[15]. R. Ali, C. P. Bhalla, C. L. Cocke, and M. Stockli, **“Dielectronic recombination on heliumlike argon”** Phys. Rev. Lett. **64**, (1990), PP. 633-.

[16]. D. A. Knapp, R. E. Marrs, M. A. Levine, C. L. Bennett, M. H. Chen, J. R. Henderson, M. B. Schneider, and J. H. Scofield, **“Dielectronic recombination of helium-like nickel”** Phys. Rev. Lett. Vol. 62, (1989), PP. 2104-2107.

[17]. J. R. Crespo Lopez-Urrutia, B. Bapat, I. Draganic, A. Werdich, and J. Ulhrich, **“First results from the freiburg electron beam ion trap freEBIT”** Phys. Scr. Vol. T92, (2001), PP. 110-.

[18]. R. Schuch, A. Barany, H. Danared, N. Elander, and S. Mannervik, **“Storage rings, a new tool for atomic physics”** *NIMPRB*, Vol. B43, (1989), PP. 411-424.

[19]. R. Schuch, W. Zong, and N. R. Badnell, **“Recombination of cooled highly charged ions with low-energy electrons”** Int. J. of Mass Spectrometry Vol. 192, (1999), PP. 225-243.

[20]. M. Beutelspachera, H. Fadil, T. Furukawac, M. Griesera, A. Nodab, K. Nodac, D. Schwalma, T. Shiraib, and A. Wolf, **“Electron cooling experiments at the heavy ion storage ring TSR”** *NIMPRA*, Vol. 532, (2004), PP. 123-128.

[21]. M. F. Gu, **“Radiative recombination rate coefficients for bare throught f-like isisequences of Mg, Si, S, Ar, Ca, Fe, and Ni”** ApJ Vol. 589, (2003), PP. 1085-1088.

[22]. N. R. Badnell, **"Radiative recombination data for modeling dynamic finite-density plasmas"** ApJS Vol. 167, (2006), PP. 334-342.

[23]. M. A. Bautista, and N. R. Badnell, **“Dielectonic recombination data for dynamic finite-density plasmas”** A & A Vol. 466, (2007), PP. 755-762.

[24]. A. Burgess, **“A General Formula for the Estimation of Dielectronic Recombination Co-Efficients in Low-Density Plasmas”**ApJ Vol. 141, (1965), PP. 1588-1590.

[25]. D.A.Verner, G.J. Ferland, **"Atomic data for asrtrophysics. I. Radiative recombination rates for H-like, He-like, Li-like and Na-like ions over a broad range of temperature"**, ApJ Vol. 103, (1996), PP. 467-481.

[26]. S. N. Nahar, **“Electron-ion recombination rate coefficients and photoionization cross sections for astrophysically abundant elements. XI. N v-vi and F vii-viii for ultraviolet and x-ray modeling”** ApJS Vol. 164, (2006), PP. 280-296.

[27]. S. N. Nahar, **“Electron-ion recombination rate coefficients and photoionization cross sections for astrophysically abundant elements. XII. Na ix, Na x, Mg x, and Mg xi for ultraviolet and x-ray modeling”** ApJS Vol. 167, (2006), PP. 315-333.

[28]. S. N. Nahar, **“Electron-ion recombination rate coefficients and photoionization cross sections for astrophysically abundant elements. IX. Ni xxvi and Ni xxvii for ultraviolet and x-ray modeling”** ApJS Vol. 158, (2005), PP. 80-92.

Table (1): The fitting parameters for ions under investigation.

ION	A($cm^3\ s^{-1}$)	B	T_0(K)	T_1(K)
F^{7+}	9.958(-11)$^{(*)}$	0.5274	3.012(3)	2.896(7)
F^{8+}	3.128(-10)	0.6712	7.227(2)	5.587(7)
F^{9+}	8.218(-10)	0.7491	2.046(2)	5.638(7)
Na^{9+}	1.393(-10)	0.5433	4.258(3)	3.872(7)
Na^{10+}	3.879(-10)	0.6718	1.133(3)	8.008(7)
Na^{11+}	9.743(-10)	0.7488	3.217(2)	8.428(7)
Mg^{10+}	1.602(-10)	0.5492	4.944(3)	4.434(7)
Mg^{11+}	4.214(-10)	0.6713	1.396(3)	9.433(7)
Mg^{12+}	1.022(-09)	0.7476	4.098(2)	1.011(8)
Ni^{26+}	4.901(-10)	0.5836	2.460(4)	1.937(8)
Ni^{27+}	1.063(-09)	0.6744	7.979(3)	4.653(8)
Ni^{28+}	2.577(-09)	0.7497	1.949(3)	5.434(8)

$^{(*)}$ the number 9.958(-11) denotes 9.958×10^{-11}

Table (2): The coefficients C_i, E_i which represent fitting parameters for ions under investigation.

ION	i	$C_i(K^{3/2}cm^3s^{-1})$	$E_i(K)$
F^{7+}	1	1.006(-02)	6.330(6)
	2	6.743(-02)	7.859(6)
	3	1.034(-02)	9.755(6)
Na^{9+}	1	2.228(-02)	9.521(6)
	2	1.133(-01)	1.195(7)
	3	1.296(-02)	1.502(7)
Mg^{10+}	1	3.067(-02)	1.136(7)
	2	1.375(-01)	1.431(7)
	3	1.347(-02)	1.762(7)

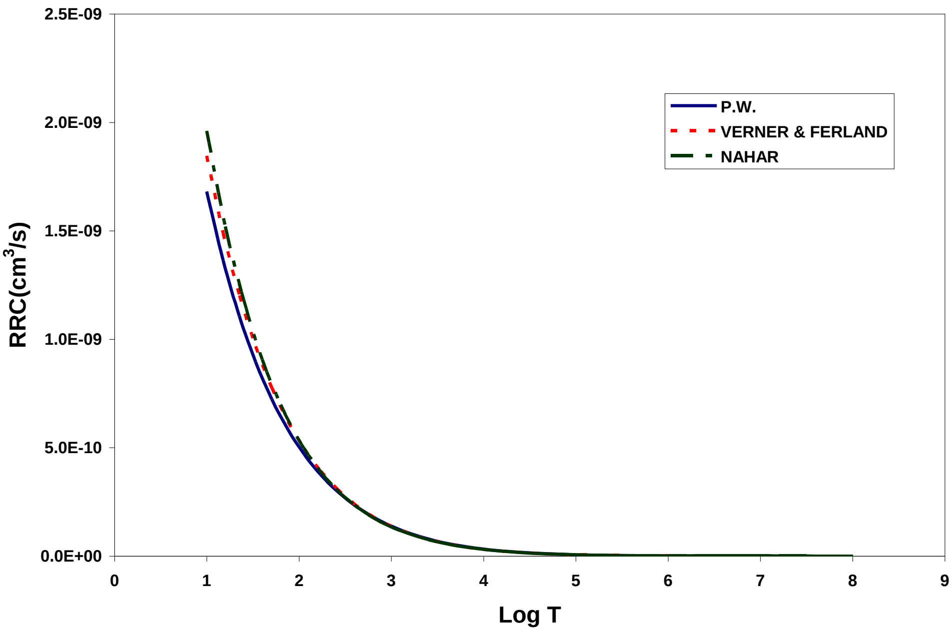

FIG.(1):Radiative recombination rate coefficient for F VII-ION compared with VERNER & FERLAND (1996) and NAHAR (2006) calculations.

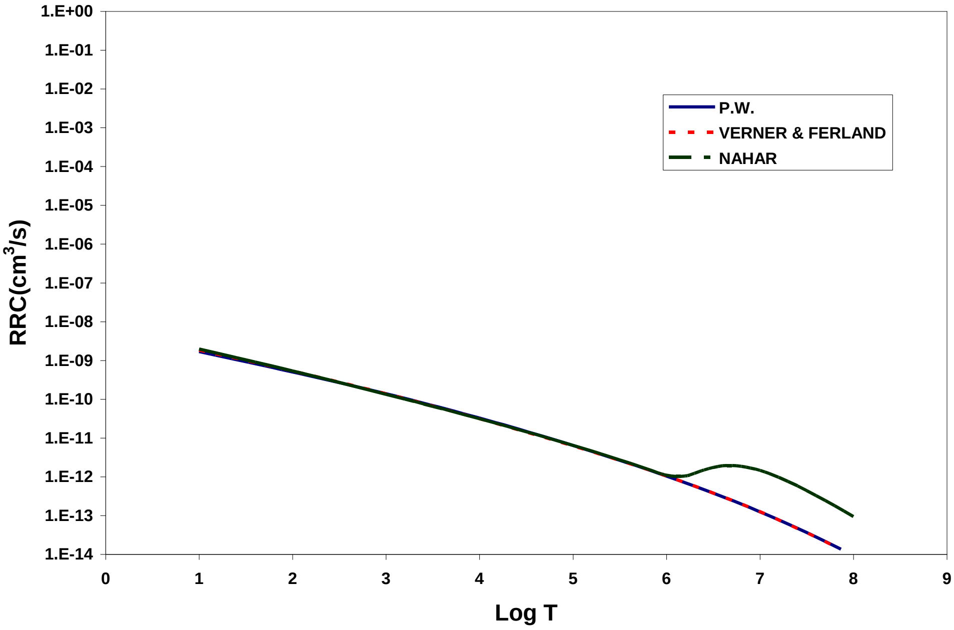

FIG.(2):The same for FIG.(1) in logarithmic scale for RRC to see the dielectronic effects arise for NAHAR at LogT>6.

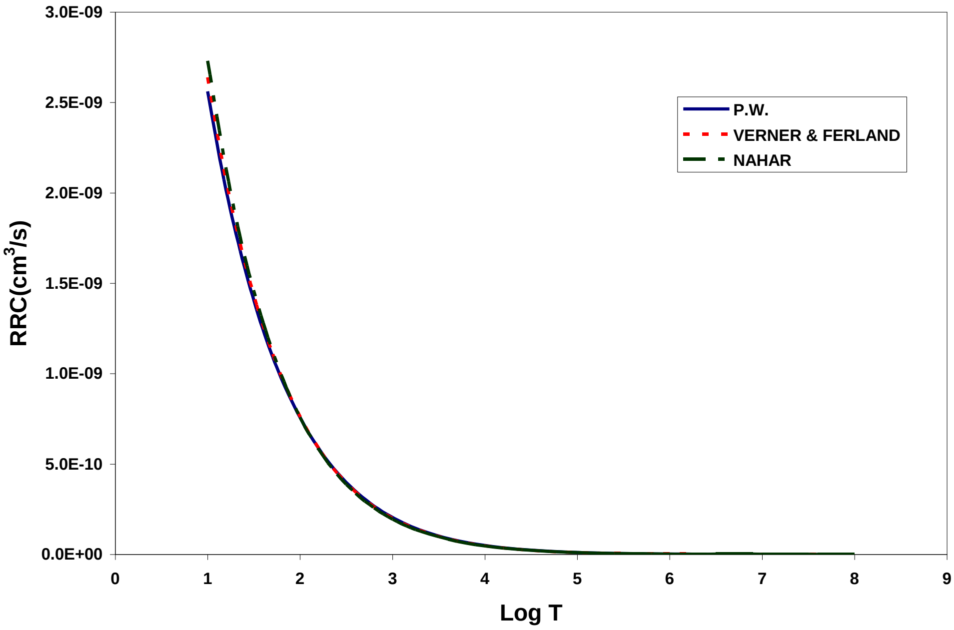

FIG.(3):Radiative recombination rate coefficient for F VIII-ion compared with VERNER & FERLAND (1996) and NAHAR (2006) calculations.

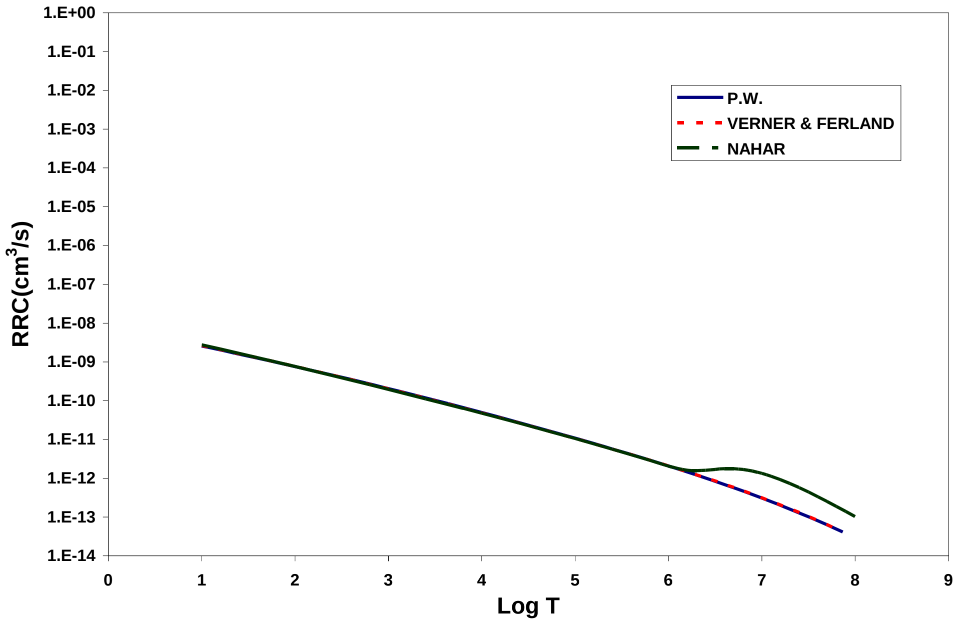

FIG.(4):The same for FIG.(3) in logarithmic scale for RRC to see the dielectronic effects arise for NAHAR at LogT>6.2

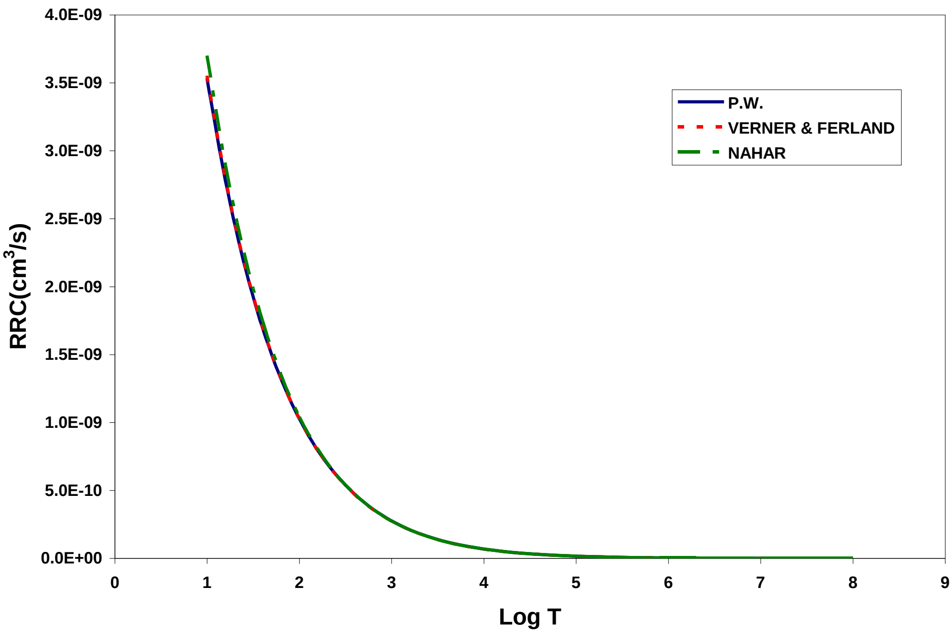

FIG.(5):Radiative recombination rate coefficient for F IX-ion compared with VERNER & FERLAND (1996) and NAHAR (2006) calculations.

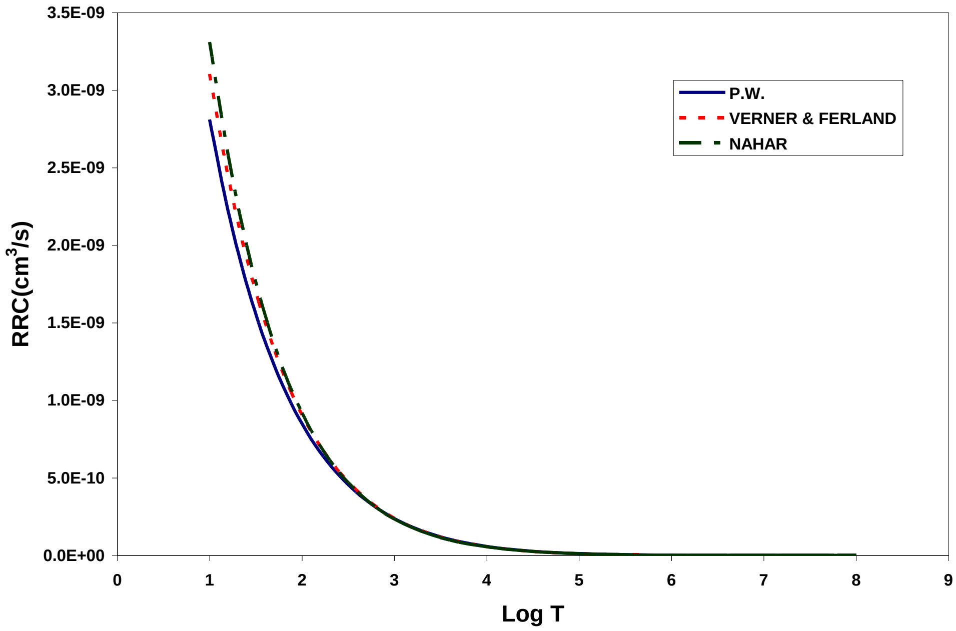

FIG.(6):Radiative recombination rate coefficient for Na IX-ion compared with VERNER & FERLAND (1996) and NAHAR (2006) calculations.

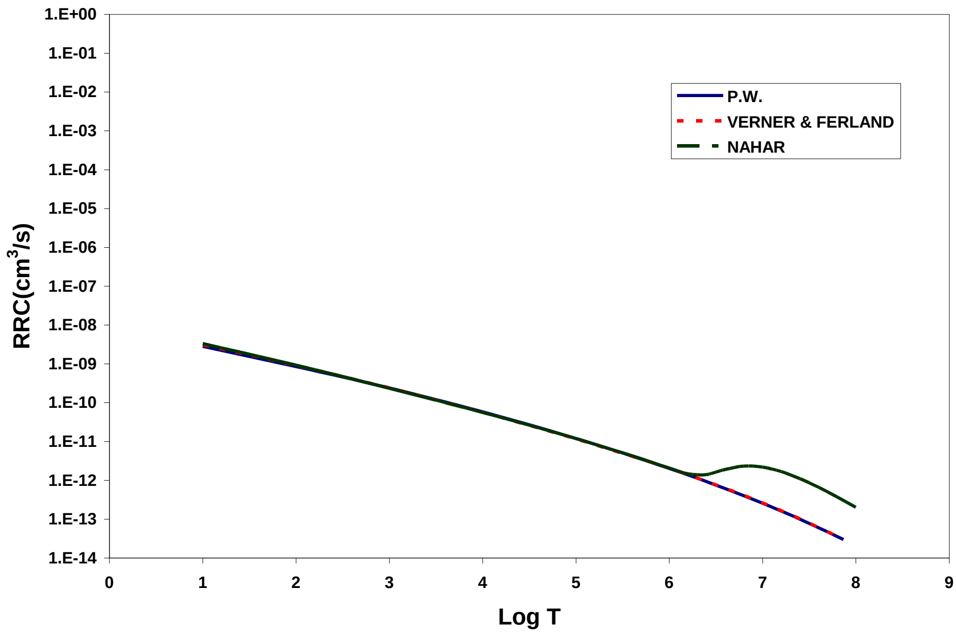

FIG.(7):The same for FIG.(6) in logarithmic scale for RRC to see the dielectronic effects arise for NAHAR at LogT>6.2

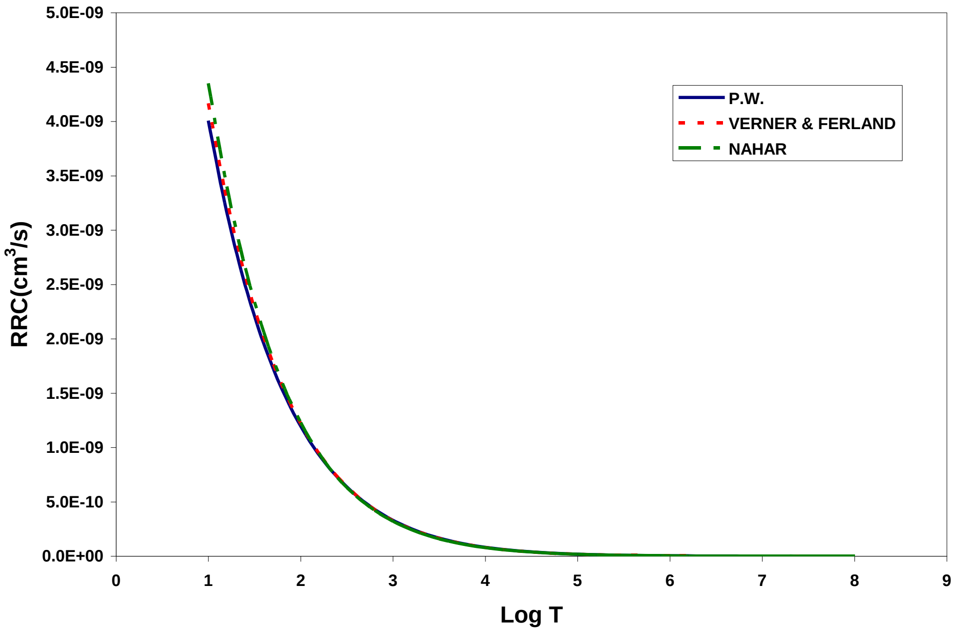

FIG.(8):Radiative recombination rate coefficient for Na x-ion compared with VERNER & FERLAND (1996) and NAHAR (2006) calculations.

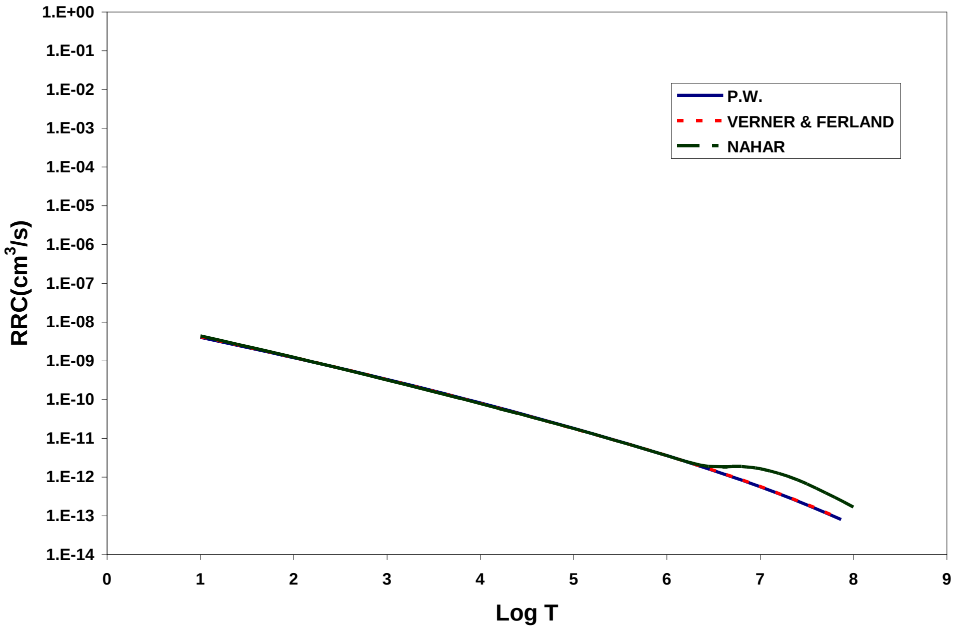

FIG.(9):The same for FIG.(8) in logarithmic scale for RRC to see the dielectronic effects arise for NAHAR at LogT>6.4

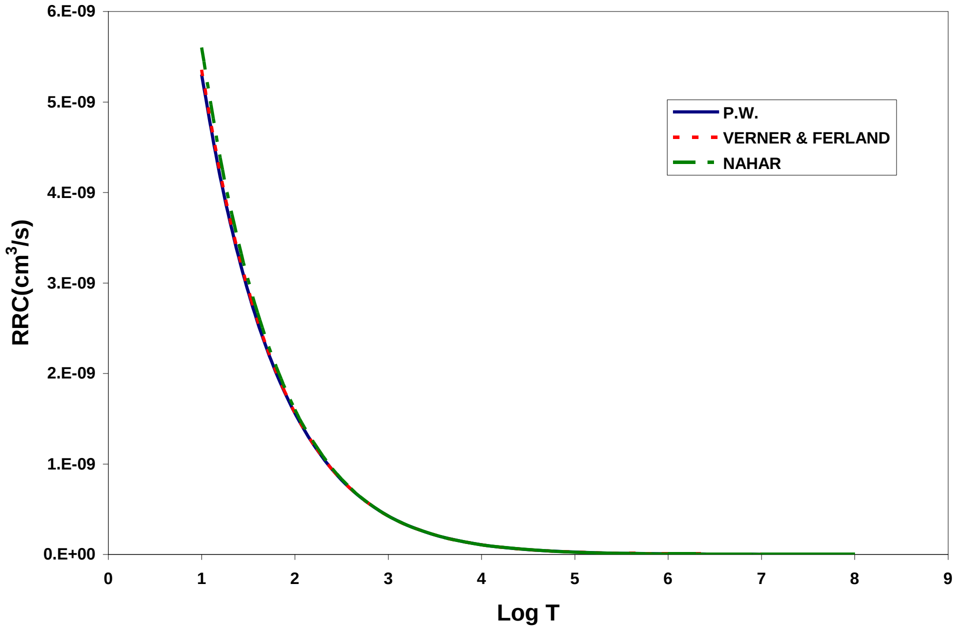

FIG.(10):Radiative recombination rate coefficient for Na XI-ion compared with VERNER & FERLAND (1996) and NAHAR(2006) calculations.

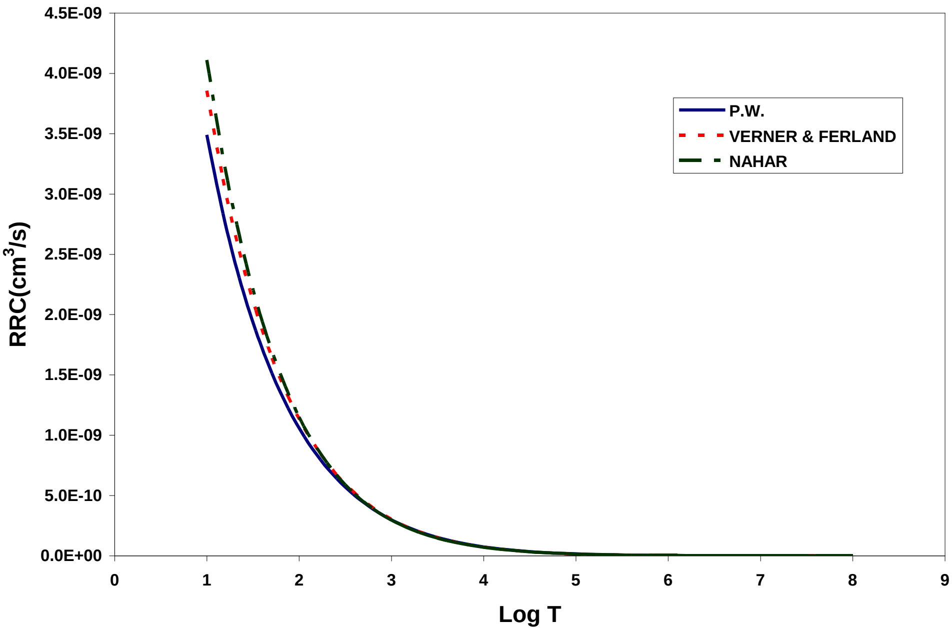

FIG.(11):Radiative recombination rate coefficient for Mg X-ion compared with VERNER & FERLAND (1996) and NAHAR (2006) calculations.

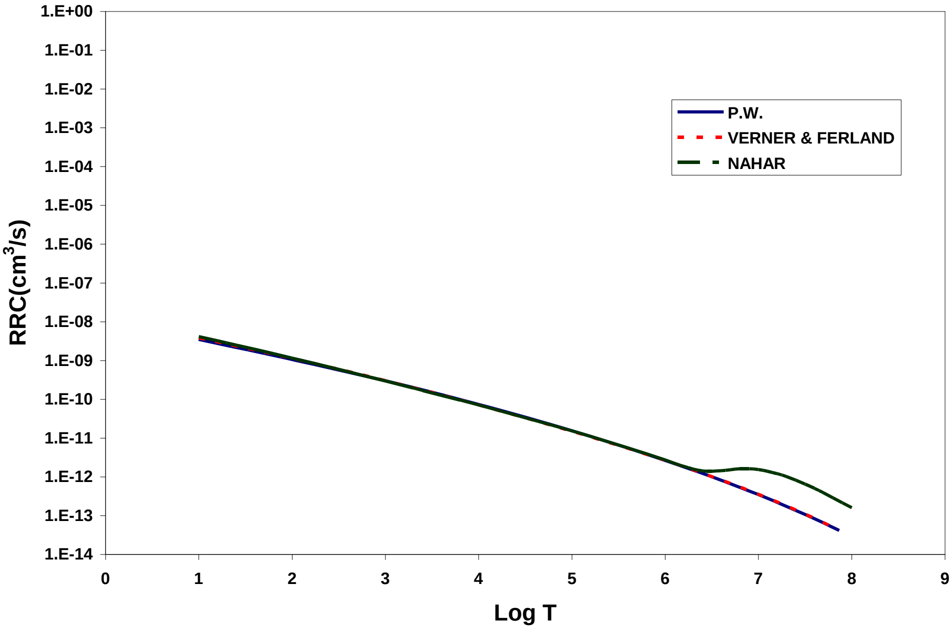

FIG.(12):The same for FIG.(11) in logarithmic scale for RRC to see the dielectronic effects arise for NAHAR at LogT>6.4

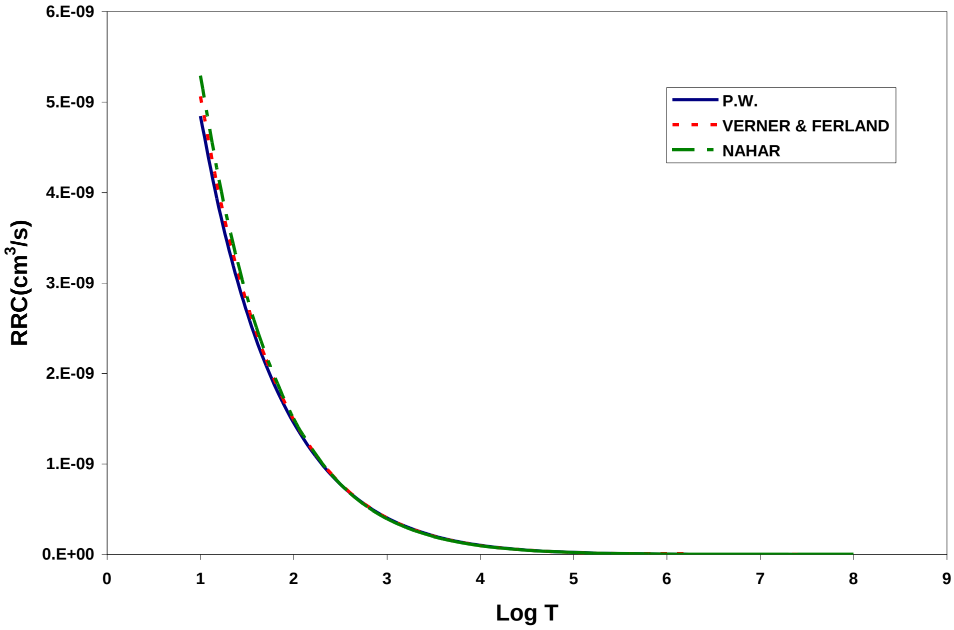

FIG.(13):Radiative recombination rate coefficient for Mg XI-ion compared with VERNER & FERLAND (1996) and NAHAR (2006) calculations.

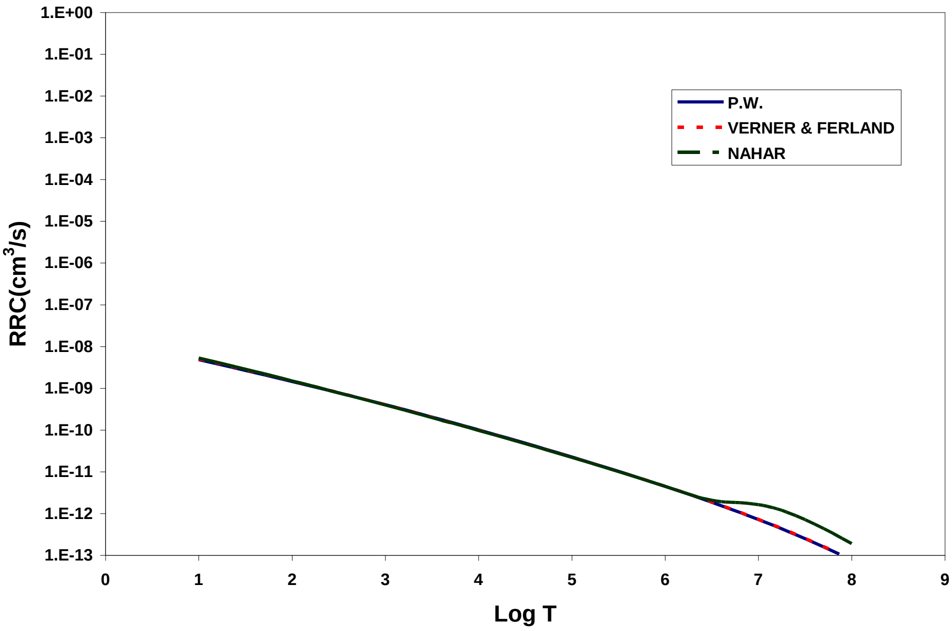

FIG.(14):The same for FIG.(13) in logarithmic scale for RRC to see the dielectronic effects arise for NAHAR at LogT>6.6

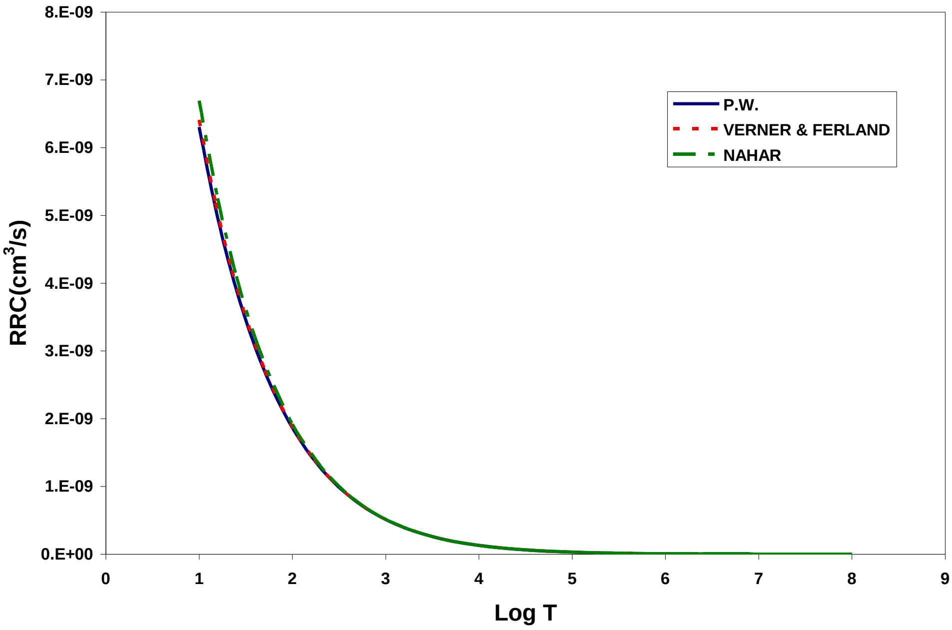

FIG.(15):Radiative recombination rate coefficient for Mg XII-ion compared with VERNER & FERLAND (1996) and NAHAR (2006) calculations.

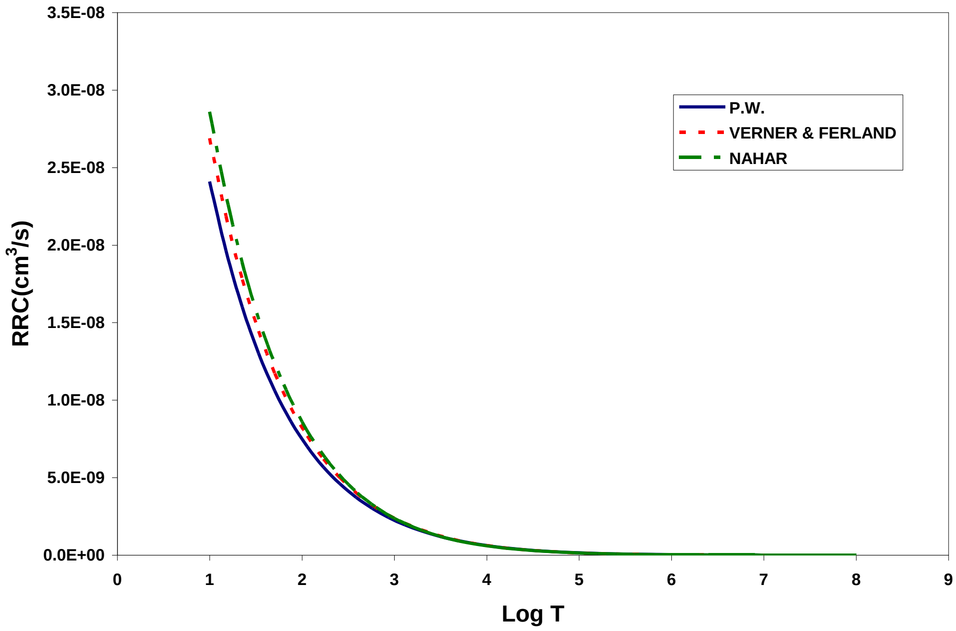

FIG.(16):Radiative recombination rate coefficient for Ni XXVI-ion compared with VERNER & FERLAND (1996) and NAHAR (2005) calculations.

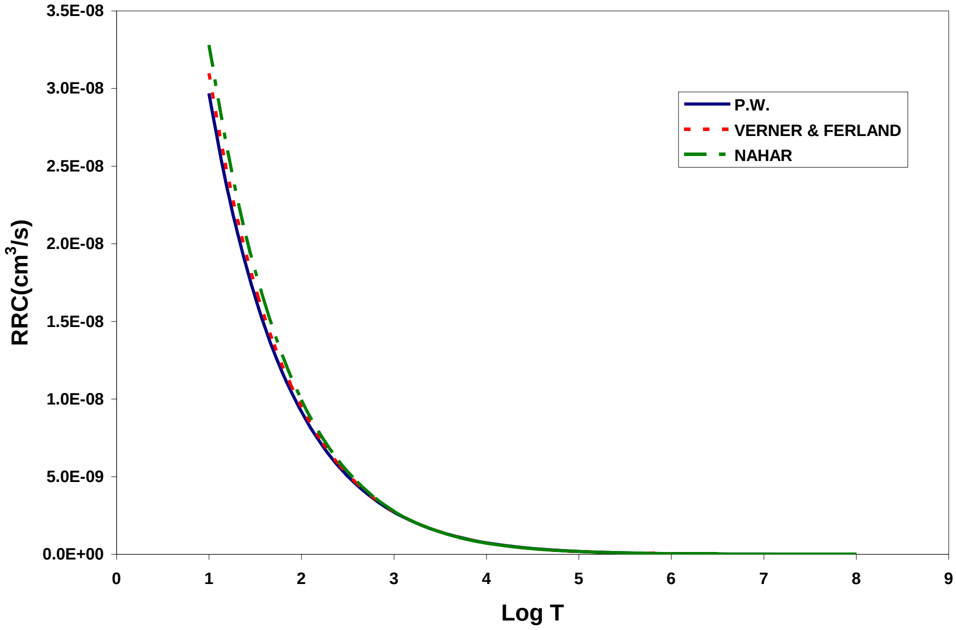

FIG.(17):Radiative recombination rate coefficient for Ni XXVII-ion compared with VERNER & FERLAND (1996) and NAHAR (2005) calculations.

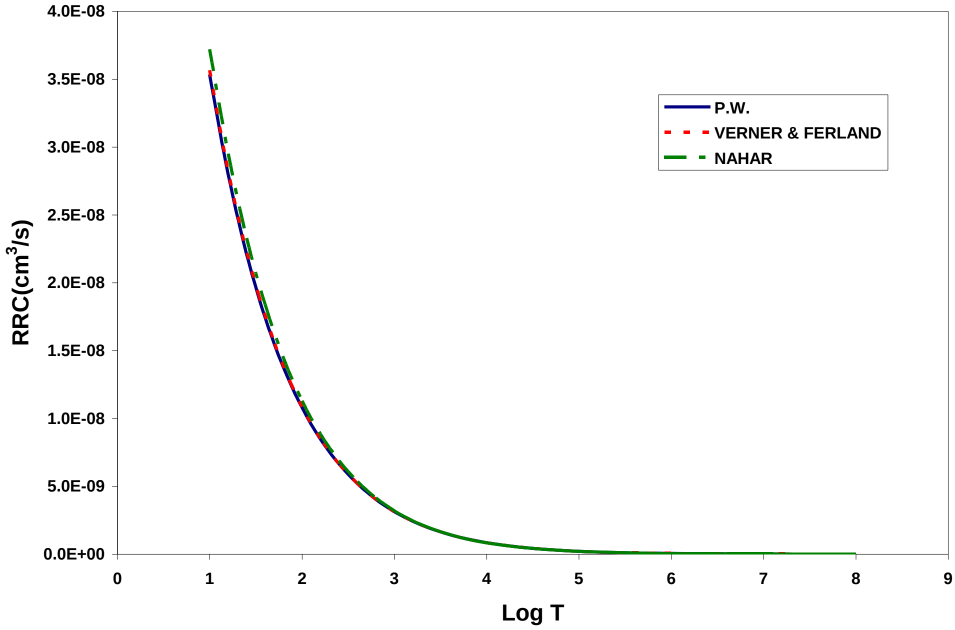

FIG.(18):Radiative recombination rate coefficient for Ni XXVIII-ion compared with VERNER & FERLAND and NAHAR calculations.

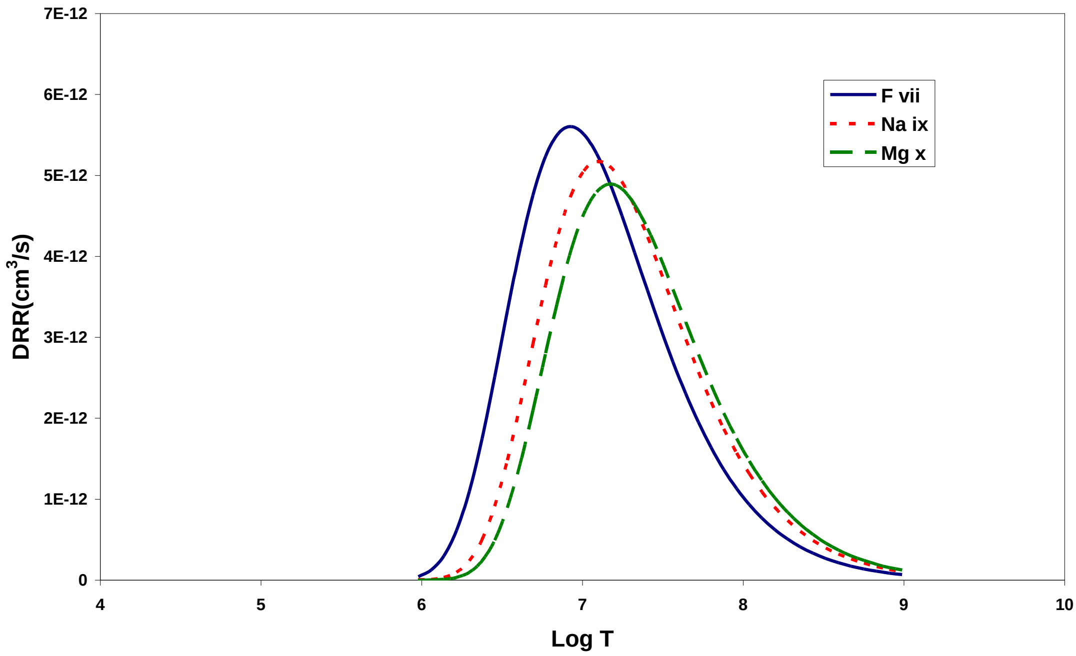

FIG(19):The dielectronic recombination rate coefficient for (F VII, Na IX, Mg X)-ions

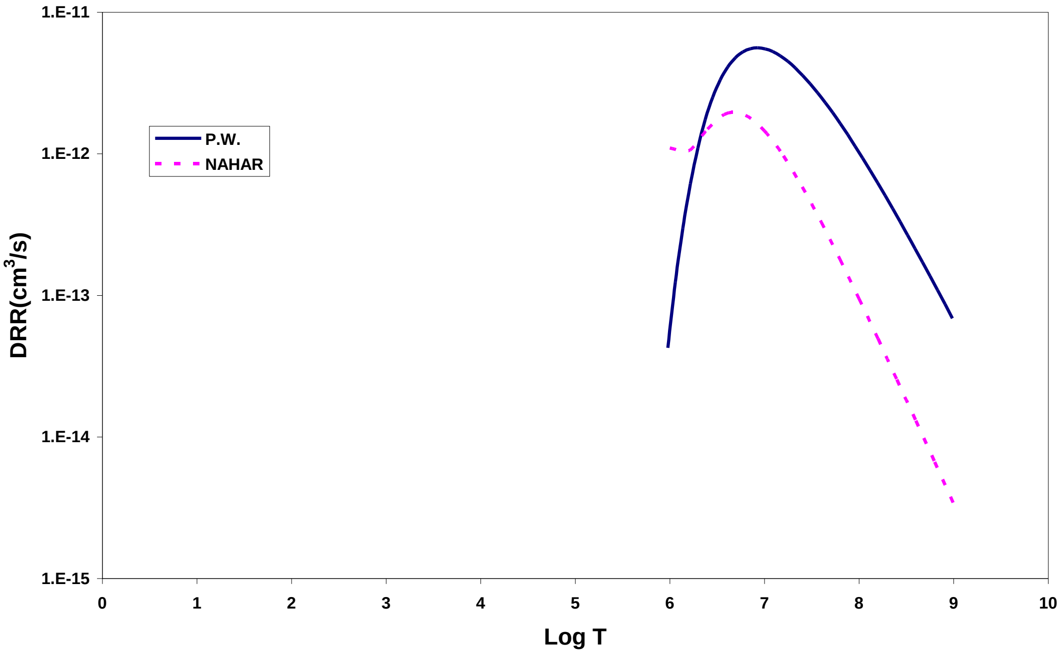

FIG.(20):The dielectronic recombination rate coefficient for F VII-ion compared with NAHAR (2006) data.

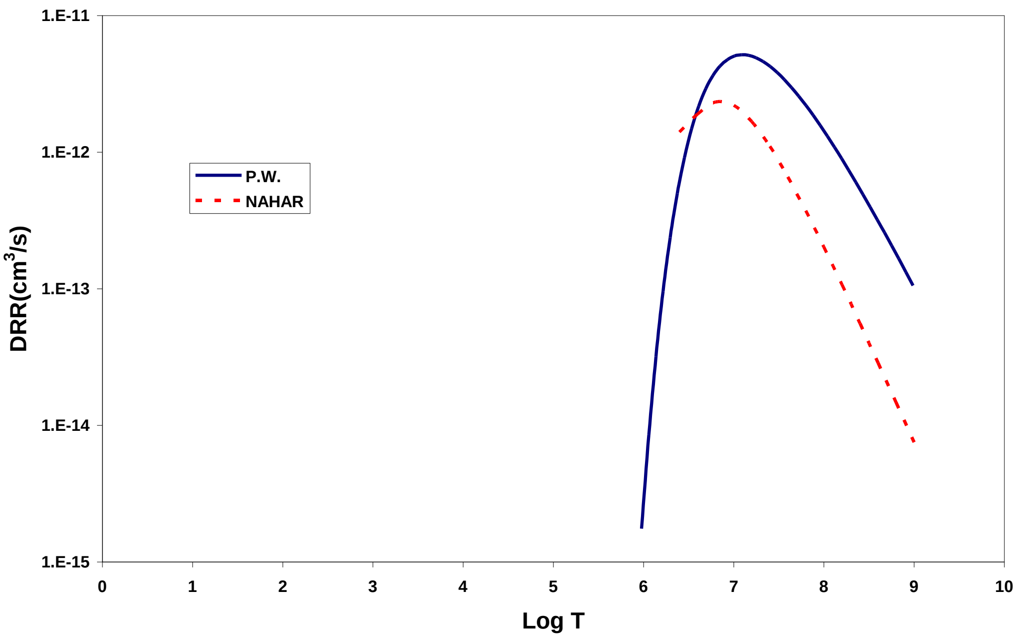

FIG.(21):The dielectronic recombination rate coefficient for Na IX-ion compared with NAHAR (2006) data

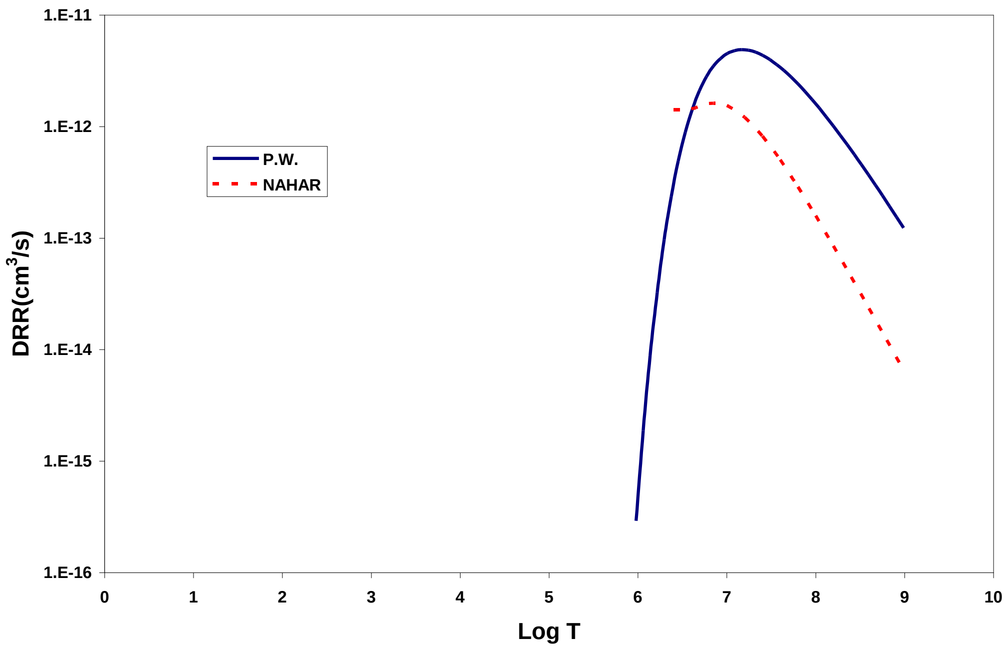

FIG.(22):The dielectronic recombination rate coefficient for Mg x-ion compared with NAHAR (2006) data